Towards Landslide Predictions: Two Case Studies

D. Sornette[1−3], A. Helmstetter[3], J. V. Andersen[1,5], S. Gluzman[3], J.-R. Grasso[3,4] and V. Pisarenko[6]

[1] LPMC, CNRS UMR 6622 and Université de Nice-Sophia Antipolis
Parc Valrose, 06108 Nice, France
[2] Department of Earth and Space Sciences
University of California, Los Angeles, California 90095-1567
[3] Institute of Geophysics and Planetary Physics
University of California, Los Angeles, California 90095-1567
[4] LGIT, Observatoire de Grenoble, Université Joseph Fourier, France
[5] U. F. R. de Sciences Economiques, Gestion, Mathématiques et Informatique,
CNRS UMR7536 and Université Paris X-Nanterre
92001 Nanterre Cedex, France
[6] International Institute of Earthquake Prediction Theory and Mathematical Geophysics
Russian Ac. Sci. Warshavskoye sh., 79, kor. 2, Moscow 113556, Russia

Abstract

In a previous work [1], we have proposed a simple physical model to explain the accelerating displacements preceding some catastrophic landslides, based on a slider-block model with a state and velocity dependent friction law. This model predicts two regimes of sliding, stable and unstable leading to a critical finite-time singularity. This model was calibrated quantitatively to the displacement and velocity data preceding two landslides, Vaiont (Italian Alps) and La Clapière (French Alps), showing that the former (resp. later) landslide is in the unstable (resp. stable) sliding regime. Here, we test the predictive skills of the state-and-velocity-dependent model on these two landslides, using a variety of techniques. For the Vaiont landslide, our model provides good predictions of the critical time of failure up to 20 days before the collapse. Tests are also presented on the predictability of the time of the change of regime for la Clapière landslide.

1 Introduction

There is a growing interest in understanding and predicting catastrophic phenomena, such as floods, earthquakes and avalanches, which are characterized by their rareness and burstiness often leading to disastrous consequences for the embedding environment [2]. Notwithstanding their large societal impacts, the scientific community is only beginning to develop the concepts and tools to model and predict these class of events. The prediction of catastrophes is often considered to be essentially impossible either due to intrinsic mechanisms inherent to the systems [3] or from the existence of enormous practical barriers [4]. Several groups have however found evidence of a degree of predictability of certain catastrophes [5], such as financial crashes [6] and earthquakes [7].

Here, we address the question of the predictability of landslides which constitute a major geologic hazard of strong concern in most parts of the world. Landslides occur in a wide variety of geomechanical contexts, geological and structural settings, and as a response to various loading and triggering processes. They are often associated with other major natural disasters such as earthquakes, floods and volcanic eruptions.

Derived from the civil-engineering methods developed for the safety of human-built structures, including dams and bridges, the standard approach to slope instability is to identify the conditions under which a slope becomes unstable [8]. By their nature, standard stability analysis cannot account for acceleration in slope movement [9]. The problem is that this modeling strategy gives a nothing-or-all signal. In this view, any specific landslide is essentially unpredictable, and the focus is on the recognition of landslide prone areas. This approach is very similar to the practice in seismology called "time-independent hazard" where earthquake prone areas are located in association with active faults for instance, while the prediction of individual earthquake is recognized to be much more difficult if not unattainable. This "time-independent hazard" essentially amounts to assume that landslides are a random (Poisson) process in time, and uses geomechanical modeling to constrain the future long-term landslide hazard. The approaches in terms of a safety factor do not address the preparatory stage leading to the catastrophic collapse, if any. In contrast,"time-dependent hazard" would accept a degree of predictability in the process, in that the landslide hazard varies with time, maybe in association with varying external forcing (rain, snow, earthquake, volcano). The next level in the hierarchy would be "landslide forecasting", which require significant better understanding to allow for the prediction of some of the features of an impending landslide, usually on the basis of the observation of precursory signals. Practical difficulties include identifying and measuring reliable, unambiguous precursors, and the acceptance of an inherent proportion of missed events or false alarms.

Our purpose is to extend the model of a slider-block with state-and-velocity-dependent friction introduced in our companion paper [1] for the analysis of two landslides. Here, we examine how one could have perhaps predicted these landslides in advance. By studying these two cases, we hope to develop a methodology that could be useful in the future as well as to determine the limits of predictability. For the Vaiont landslide, our model provides good predictions with a precision of about one day of the critical time of failure up to 20 days before the collapse. Tests are also presented on the prediction of the time of the change of regime for la Clapière landslide. Re-examining the calibration of the model of a slider-block with state-and-velocity-dependent friction, we cannot exclude that La Clapière might also belong to the unstable velocity weakening regime; its deceleration observed after 1988 may then be interpreted as a change of surface properties that modifies the friction law parameters.

2   A short synthesis of time-dependent predictive approaches

2.1   Phenomenological power law acceleration

Accelerating displacements preceding some catastrophic landslides have been found empirically to follow a time-to-failure power law, corresponding to a finite-time singularity of the velocity $v \sim 1/(t_c - t)$ [10]. Controlled experiments on landslides driven by a monotonic load increase have been quantified by a scaling law relating the surface acceleration $d\dot{\delta}/dt$ to the surface velocity $\dot{\delta}$ according to

$$d\dot{\delta}/dt = A\dot{\delta}^{\alpha} \ , \tag{1}$$

where A and α are empirical constants [11]. For $\alpha > 1$, this relationship predicts a divergence of the sliding velocity in finite time at some critical time t_c. The divergence is of course not to be taken literally: it signals a bifurcation from accelerated creep to complete slope instability for which inertia is no more negligible. Several cases have been quantified ex-post with this law, usually for $\alpha = 2$, by plotting the time $t_c - t$ to failure as a function of the inverse of the creep velocity (see

[12] for a review). Indeed, integrating (1) gives

$$t_c - t \sim \left(\frac{1}{\dot{\delta}}\right)^{\frac{1}{\alpha-1}} . \tag{2}$$

For the Mont Toc, Vaiont landslide revisited here, Voight mentioned that a prediction of the failure date could have been made more than 10 days before the actual failure, by using a linear relation linking the inverse velocity and the time to failure, as found from (2) for $\alpha = 2$ [10]. Our goal will be to avoid such an a priori postulate by calibrating a more general physically-based model for the purpose of forecasting.

2.2 Slider-Block model with state and velocity dependent friction

We briefly summarize Ref. [1], which models the future landslide as a block resting on an inclined slope forming a fixed angle ϕ with respect to the horizontal. The solid friction coefficient μ between two surfaces is taken to be a function of the cumulative slip δ and the slip velocity $\dot{\delta}$ according to the Dieterich-Ruina law [13, 14]:

$$\mu = \mu_0 + A \ln \frac{\dot{\delta}}{\dot{\delta}_0} + B \ln \frac{\theta}{\theta_0} , \tag{3}$$

where the state variable θ is usually interpreted as proportional to the surface of contact between asperities of the two surfaces. μ_0 is the friction coefficient for a sliding velocity $\dot{\delta}_0$ and a state variable θ_0. The state variable θ evolves with time according to

$$\frac{\mathrm{d}\theta}{\mathrm{d}t} = 1 - \frac{\theta\dot{\delta}}{D_c} , \tag{4}$$

where D_c is a characteristic slip distance, usually interpreted as the typical size of asperities. Expression (4) can be rewritten as

$$\frac{\mathrm{d}\theta}{\mathrm{d}\delta} = \frac{1}{\dot{\delta}} - \frac{\theta}{D_c} . \tag{5}$$

For $m \neq 1$, it is convenient to introduce the reduced variables

$$x \equiv (S\theta_0)^{1/(1-m)} \frac{\theta}{\theta_0} , \tag{6}$$

and

$$D \equiv D_c \ (S\theta_0^m)^{\frac{1}{1-m}} , \tag{7}$$

where

$$S \equiv \frac{\dot{\delta}_0 \ e^{\frac{\frac{\tau}{\sigma}-\mu_0}{A}}}{D_c} \tag{8}$$

and $m = B/A$. τ and σ are the average shear and normal stresses at the sliding interface of the block. Then, expression (3) reads

$$\frac{\dot{\delta}}{\dot{\delta}_0} = D \ x^{-m} . \tag{9}$$

Similarly, expression (4) transforms into

$$\frac{\mathrm{d}x}{\mathrm{d}t'} = 1 - x^{1-m} , \tag{10}$$

3

where $t' = t/T$ with

$$T = \frac{D_c}{D} = \left[\frac{D_c}{\dot{\delta}_0 \theta_0^m}\right]^{1/(1-m)} e^{\frac{\frac{\tau}{\bar{\sigma}} - \mu_0}{B-A}} .$$ (11)

In the sequel, we shall drop the prime and use the dimensionless time t', meaning that time is expressed in units of T except stated otherwise. The case $m = 1$ requires a special treatment [1].

In our previous companion paper [1], we have analyzed this set of equations (9,10) and shown that it provides a physical basis for the phenomenological law (2). Indeed, it is easy to show that, for $m > 1$ and $x_i < 1$ and sufficiently close to the singularity t_c, the slip velocity is of the form (2) with $\alpha = 2$, that is, the slip velocity is inversely proportional to time. Consequently, the slip $\delta(t) \sim \ln[1/(t_c - t)]$ diverges logarithmically.

More generally, depending on the ratio $m = B/A$ of two parameters of the rate and state friction law and on the initial frictional state of the sliding surfaces characterized by the reduced parameter $x_i = x(t = 0)$ defined in (6), four possible regimes are found. Two regimes can account for an acceleration of the displacement. For $B/A > 1$ (velocity weakening) and $x_i < 1$, the slider block exhibits an unstable acceleration leading to a finite-time singularity of the displacement and of the velocity $\dot{\delta} \sim 1/(t_c - t)$, thus rationalizing Voight's empirical law. An acceleration of the displacement can also be reproduced in the velocity strengthening regime, for $B/A < 1$ and $x_i > 1$. In this case, the acceleration of the displacement evolves toward a stable sliding with a constant sliding velocity. The two others cases ($B/A < 1$ and $x_i < 1$, and $B/A > 1$ and $x_i > 1$) give a deceleration of the displacement. We have used the slider-block friction model to analyze quantitatively the displacement and velocity data preceding two landslides, Vaiont (in the Italian Alps) and La Clapière (in the French Alps) [1]. The Vaiont landslide was the catastrophic culmination of an accelerated slope velocity. La Clapière landslide was characterized by a strong slope acceleration over a two years period, succeeded by a restabilizing phase. Our inversion of the slider-block model on these data sets showed good fits and suggested to classify the Vaiont (respectively La Clapière) landslide as belonging to the velocity weakening unstable (respectively strengthening stable) sliding regime.

3   Prediction of the Vaiont landslide

On October 9, 1963, a 2 km-wide landslide initiating at an elevation of 1100-1200 m, that is 500-600 m above the valley floor, on the Mt Toc slope in the Dolomite region in the Italian Alps about 100 km north of Venice, ended up 70 days later in a 20 m/s run-away of about 0.3 km^3 of rocks sliding into a dam reservoir. The high velocity of the slide triggered a water surge within the reservoir, overtopping the dam and killing 2000 people in the village downstream. For a synthesis of its history and the analysis of time series of slip velocity of benchmarks on its flanks, we refer to our companion paper [1].

3.1   Analysis of the cumulative displacement data with the slider-block model parameters

Previously, we have calibrated the slider-block model with state-and-velocity-dependent friction on the time series of slip velocities of several benchmarks. The key parameter $m = B/A$ is found to be larger than 1, indicating an unstable regime leading to a finite-time singularity [1]. However, we noted that the parameters of the friction law are poorly constrained by the inversion. In particular, even for those benchmarks with the best fit gives $m > 1$, other models with $m < 1$ provide a good fit to the velocity with only slightly larger residuals.

4

We now contrast these results with those obtained by fitting the cumulative displacement (rather than the velocity) with the slider-block model with the state and velocity friction law (9) and (10). The results are shown in Figure 1. The fitted m are respectively $m = 0.99$ (benchmark 5), $m = 0.85$ (benchmark 63), $m = 0.68$ (benchmark 67) and $m = 0.17$ (benchmark 50). These values differ significantly from those obtained by the inversion of the velocity data and, to make things worse, they all correspond to the velocity-strengthening regime $m < 1$. At first sight, these results are quite surprising since we fit the same data, the only difference being that the cumulative displacement is the integral of the velocity. We think that the reason for these discrepancies lies in the fact that, assuming that the velocity-weakening regime $m > 1$ holds, the corresponding logarithmic dependence $\delta(t) \sim \ln(1/t_c - t)$ of the displacement δ is extremely degenerate in that it predicts an acceleration of the displacement which is significant only very close to the critical time t_c. Therefore, a cross-over from a low velocity to a larger velocity described by the regime $m < 1$ may be selected by the inversion, as we witness here. This is a rather standard problem of logarithmic singularities, which are so weak at providing constraints, notwithstanding the a priori reduction of noise obtained by constructing a cumulative quantity. It may actually be the case that the cumulative noise deriving from the integral of the velocity is enough to spoil the weak logarithmic singularity [15]: the resulting correlated noise seems to select a milder behavior. We are thus led to conclude that fits to the sliding velocity which involves stronger power law singularities should be more reliable and we shall use them exclusively in our prediction tests reported for the Vaiont landslide.

3.2   Initiation of the instability and tests of robustness

The critical acceleration is observed neatly only in the last 70 days before the catastrophic landslide. Before, the alternation of phases of accelerating and decelerating velocity in the 1960-1962 period implies that some friction parameters have changed, maybe due to changes in water level, resulting in a change of sliding regime. The change of water level may have modified the material properties of the underlying solid contacts at the base of the moving rock mass [16], therefore changing the parameter $m = B/A$ from the stable to the unstable regime. Another possibility is that changes in water level have modified the population of contacts at the basis of the rock mass, therefore changing the parameters of the friction law, and changing the sliding regime from the decelerating regime to to the accelerating regime. One possible simple change of the parameters of the friction law correspond to a change of the initial condition on the state variable x_i, which may induce a change of the sliding regime from the decelerating regime for $m > 1$ and $x_i > 1$ to the accelerating regime for $m > 1$ and $x_i < 1$ and vice-versa.

We have also tried to invert the friction law parameters using only data up to a time t_{max} smaller than the last available point (equal to 70 days from the origin of the time series) before the catastrophic landslide occurs, to mimic a real-time situation. Changing t_{max} between 30 and 70 days, we obtain a large variability of the parameters. Most values m are found larger than 1 for $30 < t_{max} < 55$ days, and then become smaller than one, and return to $m \geq 1$ for 3 benchmarks when using the full velocity data. Similar fluctuations are found when using a synthetic data set generated with the friction model. We have generated a synthetic data set using the same parameters as those of the best fit of benchmark 5, and added a white noise with the same standard deviation as that of the residue of the fit of benchmark 5. Although this synthetic data set was generated with $m = 1.35$, both $m > 1$ and $m < 1$ (for 2 points over 15 points) values are obtained when inverting the parameters up to t_{max} and changing t_{max} between 30 and 70 days. However, values with $m < 1$ for this synthetic data set are much less frequent than for the Vaiont velocity data in relative terms.

3.3 Predictions and ex-post skills

We present a series of attempts at predicting in advance the critical time t_c of the catastrophic Vaiont landslide instability. These attempts rely solely on the analysis of the four benchmarks velocity data up to various times $t_{\max} < t_c$ mimicking a real-time situation. Therefore, we truncate the data at some time $t_{\max} < t_c$ and use only the data up to $t_{\max}$. Our goal is i) to investigate whether a prediction in advance could have been issued, as suggested by Voight [10], ii) to establish the reliability and the precision limits of such predictions and iii) to test various prediction schemes that we have developed in the recent past for other applications or specifically for this problem. We use and compare three methods to predict the critical time $t_c = 69$ days of the collapse

- the slider block model with the state and velocity friction law described above;

- an approximation of the slider block model based on the functional renormalization method described below;

- a simple finite-time singularity (2) with $\alpha = 2$ as proposed by Voight [10].

3.3.1 Prediction using the slider-block model with the state and velocity friction law

The prediction of the critical time t_c is obtained by fitting the slider-block model on the velocity time series of the four benchmarks up to a time $t_{\max}$. For $m \geq 1$, t_c is the time of the divergence. The divergence of the velocity exists only in the unstable regime $m > 1$. Therefore, we choose the best fit with $m > 1$, even if the best model gives sometimes $m < 1$.

3.3.2 Functional renormalization of the friction law

We are dealing with a noisy time series with relatively few data points for which the detection of a singularity is a difficult task. Rather than using the full solution of a model assumed to be a good representation of reality as done in the previous sections, it may be profitable to develop prediction schemes that are less constrained by the necessarily restricting physical assumptions underlying the model and that are more specifically designed from a mathematical point of view to be resilient to noise and to the scarcity of data. Such a method is the so-called functional renormalization method, which constructs the extrapolation for future time $t > t_{\max}$ from a re-summation of the time series represented by a simple polynomial expansion in powers of time t. Its mathematical foundation has been developed in a series of papers [17, 18, 19]. The application of this method to detect and predict finite-time singularities has been already investigated in [20, 21]. We refer to these papers for a presentation of the method and restrict ourselves here to the concrete application of the method to the friction law (9) and (10).

The first input of the functional renormalization approach is an expansion of the variable to be predicted in increasing powers of time. In our case, we use the functional renormalization approach to provide an approximate analytical solution of the differential equation of the friction model (10). This method is much more efficient numerically than the numerical resolution of the differential equation (10). The friction model (10) gives the time evolution of the state variable from which the sliding velocity $\dot{\delta}$ derives using (9).

The needed expansion of $y \equiv \theta/\theta_0$ in powers of time t is obtained from a Taylor expansion whose coefficients are derived from successive differentiation of (10). Up to fourth order t^4, calling $y_0 = \theta(t = 0)/\theta_0$, we obtain

$$y_k(t) \simeq \sum_{n=0}^{k} a_n t^n, \quad t \to 0, \quad k = 1, 2, 3, 4, \tag{12}$$

6

where the coefficients a_n are given in the Appendix A as a function of the friction parameters and of the initial condition.

The functional renormalization approach is in principle able to derive an extrapolation to the future from the form (12). However, in order to obtain an optimal stabilization, it is essential to incorporate as much available information as possible. In particular, in our case, we know the functional form of the dependence of the state variable as a function of time in the asymptotic regime (large times for $m < 1$ and close to the singularity for $m > 1$). Therefore, the second input of our implementation of the functional renormalization approach is the following. For $m < 1$, in a long-time limit, it is easy to show that equation (10) has an asymptotic solution in the form,

$$ y_{t \to \infty}(t) \simeq y^* + A_1 \exp\left(-\frac{t}{t^*}\right) + A_2 \exp\left(-\frac{2t}{t^*}\right) + \text{h.o.t.} \tag{13} $$

where $1/t^* = (1 - m)/T = (1 - m)(S\theta_0)^{1/(1-m)}$ and h.o.t. stands for higher-order terms. The coefficients A_1 and A_2 are unspecified at this stage and can be determined using the crossover technique [19], in order to optimize the stability of the solution. For $m \geq 1$, the asymptotic expression as $t \to t_c$ is of the form

$$ x(t) \simeq m^{\frac{1}{m}} (t_c - t)^{\frac{1}{m}} , \tag{14} $$

where the critical time t_c is given by expression (33). However, we shall allow the prefactor and t_c to be adjusted to ensure maximum stability. Specifically, the determined value of t_c will be a primary result of the crossover technique.

Our goal is thus to construct a function $y(t)$ which incorporates the short and long time asymptotics of the solution as given by expressions (12) and (13) for $m < 1$ and by (12) and (14) for $m \geq 1$, while possibly departing from it at intermediate times to allow for a maximum stability. The general mathematical formulas that are the solution of this problem are given in Appendix A for the two cases $m < 1$ and for $m \geq 1$ respectively.

For the application to the Vaiont landslide, and for each "present time" $t_{\max}$, we assume that $m > 1$ so that t_c exists and we fit the expression of the fourth-order approximate $y_4^*(t)$ given by (32) to the velocity of each of the four benchmarks, extract the corresponding parameters and put them in equation (33) in Appendix A for the critical time t_{c4}. We stress that the function thus reconstructed is essentially indistinguishable from the fit with the slider-block friction model. Solving (33) for t_{c4} allows us to construct the predicted critical time as a function of the "present time" $t_{\max}$. We also estimate the value of m as a function of $t_{\max}$. Apart from some large jumps that may be attributed to the sensitivity of specific noisy points as $t_{\max}$ is scanned, we observe that most fits are compatible with a value of m in the range $1.3 - 1.5$.

3.3.3 Finite-time singularity (2) with $\alpha = 2$

We use a simple linear regression of the inverse of the velocity as a function of time, as proposed by Voight [10]. We have found that, in order to have more stable parameters, it is necessary to give less weight to the early times where the velocity is small and contains little information on the critical time. We find that weighting each data point proportionally to its velocity provides stable fits. The critical time t_c is then given as the time at which the fitted straight line of the $1/\dot{\delta}$ data intersects with the time axis. Recall that a linear relation between $1/\dot{\delta}$ and time t is equivalent to a power law singularity of the velocity $\dot{\delta} \sim 1/(t_c - t)$, as discussed previously, which is expected asymptotically close to t_c for the friction model in the case $m > 1$ and $x_i < 1$.

3.3.4 Comparison of three different methods of prediction of t_c as a function of the "present time" $t_{\max}$

The predictions of the critical time obtained from the three methods are shown in Figure 2. A prediction for t_c with an uncertainty of a few days is obtained for the 4 benchmarks within 20 days before the catastrophic failure. The reliability of the prediction is confirmed by the coherence and agreement between the three methods. Starting approximately at $t_{\max} = 45$ days, one can observe that, using the friction model, all four time series provide a reasonable t_c prediction which however tends to increase and to follow the value of the "present time" $t_{\max}$. This is unfortunately a common feature of fits to power law singularities in which the last data points close to the "present" tends to dominate the rest of the time series and produce a predicted time of singularity close to the "present time" $t_{\max}$ [15, 22]. The t_c value obtained using the fourth-order approximate is always a little smaller than the t_c estimated from the exact friction model. The renormalization method is therefore a little better at early times, but the exact friction model works better at the end. The t_c value obtained by the linear regression of $1/\dot{\delta}$ is too large for small t_{max}, because it is only an asymptotic solution of the friction model for $t \approx t_c$. However, this method provides very good estimates of t_c close to t_c.

To test whether the relative value of these three methods result from a genuine difference in their stability with respect to noise or rather reflects an inadequacy of the slider-block friction model to fit the data, we have generated a synthetic velocity time series obtained by using the slider-block friction equations with the same parameters as found in the fit to the full data set of benchmark 5 and adding white noise with the same standard deviation as that of the real data set. We then applied the three prediction methods to this synthetic data set. In principle and by construction, we should expect a priori that the prediction based on the slider-block friction model should always perform best since it is the *true* model. This is not what we find, as shown in Figure 3. At times far from t_c, i.e. 40 days $< t_{max} < 60$ days, the friction model is the best, as expected. However, the prediction based on the asymptotic linear relation between $1/\dot{\delta}$ and time t is slightly better than the friction model, starting approximately 9 days before the landslide.

The overall conclusion is that the least sophisticated approach, that is the linear regression of $1/\dot{\delta}$, seems to perform as well as or slightly better than the sophisticated renormalization method or the exact friction model for "present times" sufficiently close to the critical time t_c. For times further away from t_c, the renormalization method and the exact friction model are better. Although the corresponding power-law is only an asymptotic solution of the friction model for times close to t_c, the linear regression of $1/\dot{\delta}$ gives significantly better predictions than the exact model or the renormalization method. However, we must keep in mind that the use of the linear regression of $1/\dot{\delta}$ as a function of time contains two hidden and rather strong assumptions: the power law and the value of its exponent. Without the slider-block friction model, these assumptions are just guesses and are a priori unjustified.

4 Prediction of the aborted 1986-1987 peak acceleration of La Clapière landslide

We now report results on another case which exhibited a transient acceleration which did not result in a catastrophic failure but re-stabilized. This example provides what is maybe an example of the $m = B/A < 1$ stable slip regime as interpreted within the friction model. La Clapière landslide is located at an elevation between 1100 m and 1800 m on a 3000 m slope high. The volume of mostly gneiss rocks implied in the landslide is estimated to be around 50×10^6 m^3. The rock mass started to be active before the beginning of the 20th century. The displacement rate measured by aerial photogrametric survey increased from 0.5 m/yrs in the 1950-1960 period to 1.5 m/yrs

in the 1975-1982 period [23]. Starting in 1982, the displacements of 43 benchmarks have been monitored on a monthly basis using distance meters [23, 24, 25]. The displacement data for 5 benchmarks is shown in Figure 4. The velocity is shown in Figure 5. The rock mass velocities exhibited a dramatic increase between January 1986 and January 1988, that culminated in the 80 mm/day velocity during the 1987 summer and to 90 mm/day in October 1987. The homogeneity of benchmark trajectories and the synchronous acceleration phase for most benchmark, attest of a global deep seated behavior of this landslide [23]. However, a partitioning of deformation occurred, as reflected by the difference in absolute values of benchmark displacements (Figure 4). The upper part of the landslide moved slightly faster than the lower part and the NW block. The observed decrease in displacement rate since 1988 attest of a change in landsliding regime at the end of 1987 (Figure 4).

4.1 Correlations between the landslide velocity and the river flow

The velocity displays large fluctuations correlated with fluctuations of the river flow in the valley as shown in Figure 6. There is a seasonal increase of the slope velocity which reaches a maximum $V_{\max}$ of the order of or less than 30 mm/days. The slope velocity increases in the spring due to snow melting and over a few days after heavy precipitations concentrated in the fall of each year [23, 25]. During the 1986-1988 period, the snow melt and rainfalls were not anomalously high but the maximum value of the velocity, $V_{\max} = 90$ mm/day, was much larger that the velocities reached during the 1982-1985 period for comparable rainfalls and river flows [23, 24]. This strongly suggests that the hydrological conditions are not the sole control parameters explaining both the strong 1986-1987 accelerating and the equally strong slowdown in 1988-1990. During the interval 1988-1990, the monthly recorded velocities slowed down to a level slightly higher than the pre-1986 values. Since 1988, the seasonal variations of the average velocity never recovered the level established during the 1982-1985 period [24, 26]. *Rat* [27] derives a relationship between the river flow and the landslide velocity by adjusting an hydrological model to the velocity data in the period 1982 to 1986. This model tuned to this time period does not reproduce the acceleration of the velocity after 1986.

In order to study quantitatively the effect of the precipitations on the landslide velocity, we need to remove the long-term fluctuations of the velocity that may not be correlated to changes in the precipitations. Before applying a spectral analysis of the velocity data, we use simple functions to fit the displacement data. We then subtract this long-term trend to obtain stationary residuals that can be used to perform a spectral analysis of the fluctuations of the velocity. We divide the data of benchmark 10 of La Clapière into three different intervals: $[1982.917, 1987.833]$, $[1987.833, 1991.25]$ and $[1991.25, 1995.5]$. The initial values of the time and of the displacement are fixed to 0 at the beginning of each time period. In the first interval, the velocity rises (with fluctuations); in the second interval, the velocity decreases (with fluctuations); in the third interval, the velocity fluctuates around a constant. We used non-linear Least-Square fits with different fitting functions separately within each interval. The results of the fits are the following.

1. In the first interval $[1982.917, 1987.833]$, we fit the displacement by $d(t) = a(|1-t/t_0|^{-b}-1)$ with $a = 8.96, b = 1.01$ and $t_0 = 6.26$ years.

2. For the second interval $[1987.833, 1991.25]$, we use the same functional form with $a = 10.42, b = 0.4106$ and $t_0 = -0.1081$. The negative value of t_0 implies a decay of the displacement.

3. For the third interval $[1991.25, 1995.5]$, we use a fit by $d(t) = at^b$ which has only two parameters $a = 7.4687$ and $b = 0.989$.

9

The goodness of fit is very good in all three regimes: the standard deviations of the residuals being of the order of 0.4 while the magnitude of the displacement is about 30, this yields a signal-over-noise ratio of 75, which is very good.

Figure 7 compares the Burg's power spectrum of the flow rates of the Tinée river and of the detrended velocity residuals. The Burg spectrum is a smoothed FFT (fast-Fourier transform) obtained by approximating the true spectrum by that of an autoregressive process of a finite order. The top panel of figure 7 exhibits the Burg's power spectrum of the flow rates of the Tinée river on the 1982-1988 and on the 1988-1996 periods, which are proxies of the cycle of precipitations and snow melting. The bottom panel of figure 7 shows the Burg's power spectrum of the detrended velocity residuals for these two periods.

In the first time interval 1982-1988, a strong peak at the period of 1 year appears both for the velocity residuals and for the river flow. This correspondence is confirmed by the strong cross-correlation between the river flow and the landslide velocity, which is also directly apparent visually in Figure 6. We now use the language of system theory and consider the river flow as an input (or a forcing) and the landslide velocity as an output of the system. These observations of a common spectral peak and of a strong cross-correlation are then compatible with a view of the system as being linear or only weakly non-linear.

In contrast, the (linear) correlation between the river flow input and the landslide velocity output disappears in the second time interval 1988-1996, as can been seen from the absence of a spectral peak at the period of 1 years and a very weak peak at the period 6 months ($f = 2$ year^{-1}) in the (output) landslide velocity spectrum compared with the two strong peaks at the same periods of 1 years and 6 months observed in the (input) river flow spectrum. This breakdown of linear correlation seems to be associated with the birth of a strong peak close to the sub-harmonic period of 2 years ($f = 0.5$ year^{-1}), which is absent in the river flow rate. This suggests the following interpretation. Frequency doubling or more generally frequency multiplications are the results of simple nonlinearities. Indeed, higher frequency overtones in river runoff is very common feature of hydrological regime [28]. In contrast, the creation of sub-harmonics requires bifurcations or period-doubling, for instance involving nonlinear processes with time delays. It thus seems that the input of rain and snow melting is transformed by the system during the second time interval via the process of such delayed period-doubling nonlinearities. It is intriguing that the change of sliding regime to a reduction of velocity in the second time interval seems here to be associated with such a sub-harmonic non-linearity, which could be the result of a change of topology of the block structures (through fragmentation) and of the solicitation of novel fresh surfaces of sliding.

It would also be interesting to add a periodic forcing to our models to better capture the time-dependence of the velocity and study its possible nonlinear consequences. This is left for a future work, together with a complete description of the three time intervals by the slider-block friction model.

4.2   Prediction of La Clapière change of sliding regime in 1983-1988

Our previous analysis of the calibration of the frictional model to the displacement of La Clapière data finds that $m = B/A$ is very close to but smaller than one, while the value of x_i is significantly larger than 1. The corresponding fit of the displacement data with the slider-block model is shown in figure 8. This argues for La Clapière landslide to be in the stable regime [1]. However, the transition time (defined by the inflection point of the displacement) is found to increase with $t_{\max}$ as shown in figure 9. This may argue for a change of regime from an acceleration regime to a restabilization before the time $t = 1988$ of the velocity peak (corresponding to the inflection point). The parameters S and x_i found in this analysis are also poorly constrained. Similar results are obtained for different benchmarks.

The analysis of the velocity data seems to reinforce somewhat the idea of a change of regime from an unstable to a stable phase, as shown in figures 10 and 11: the early acceleration was in the unstable regime $m > 1$ but did not reach the instability due to a change of morphology, block partition and the creation of new active surfaces of sliding. This interpretation is suggested in particular by the plot of the inverse of the velocity shown in Figure 11, which is close to linear at early times. Over the route toward the finite-time singularity, the landslide perhaps did not succeed in accommodating the velocity increase and degenerated by changing geometry and loading conditions (block partitioning). In other words, the solution shown in Figure 8 with $m < 1$ may rather describe a transient from an unstable state to a stable regime. In particular, we cannot exclude the possibility that the surfaces have all along been characterized by the regime $B > A$ and then a change of geometry and surfaces of sliding may have reset the reduced state variable x given by expression (6). Another possibility is that the friction parameter m has changed from $m > 1$ to $m < 1$, leading to a stable deceleration of the displacement after 1988. It is not unreasonable to conjecture that the internal stresses associated with and created by the accelerating phase may have led to its fragmentation into several sub-entities, creating fresh surfaces and resetting the state variable or the m-value characterizing the surfaces of contact. This is in qualitative agreement with field observations of new faulting patterns since 1987, which signal a change in the geometry of the landslide involving the regression of the main scarp and locked sub-entities [24, 29]. These observations provide evidence for a change in both the head driven force (mass push from the top) and the activated basal surfaces. These morphological changes suggest that the 1987-1988 period has been a transition period for the evolution of La Clapière sliding system over the last 50 years. In the block-slider model, this amounts to modifying the variables S and θ_i and thus to reset x. In this interpretation, the change of regime observed for La Clapière could then be due to a change from $x_i < 1$ (unstable acceleration) to $x_i > 1$ (stable deceleration). This change from $x_i < 1$ to $x_i > 1$ may be interpreted as either an increase of applied shear stress, a decrease of normal stress, or an increase of the surface of contacts between the sliding surfaces. Thus, within the slider-block model, one can characterize the post 1988 landslide evolution in terms of new sliding surfaces being mobilized which are more stable that the previous ones due to more numerous and/or efficient contacts.

Appendix B explores what would have been the predicted critical time t_c estimated in real time prior to the velocity peak, according to this scenario of an unstable acceleration towards a finite-time singularity. We have seen that, while the slider-block model as well as the power law formula (2) provide excellent fits to the data, they do not lead to very stable predictions of the critical time t_c on the Vaiont data as well as on synthetic tests generated in the unstable regime $m > 1$. It may thus be valuable to test the approach of Gluzman et al. [20] in terms of a version of the functional renormalization approach already discussed in relation with the Vaiont landslide. It is our hope that this approach could provide in a more robust determination of t_c.

Figure 12 compares the prediction of a fit using a polynomial of order two in time to the inverse of the velocity (panel (a)) with the prediction of the renormalization approach (panel (b)). In each panel, two curves are presented corresponding to two different starting points of the data taken into account in the predictions: the points to the left correspond to the first date taken into account in the predictions; therefore, the predictions corresponding to the crosses $\times$ use approximately two years fewer data than the predictions shown with the open circles. This allows us to compare the effect of missing data or alternatively the effect of a non-critical behavior at the beginning of the time series. The abscissa $t_{\max}$ is the running "present time", that is, the last time of the data taken into account to issue a prediction. The prediction with the polynomial shown in panel (a) of Figure 12 can be seen as an improvement in methodology over the Voight formula (2) which corresponds to a linear fit of the inverse velocity with time for $\alpha = 2$. Comparing panels (a) and (b), the renormalization method seems to present a smaller dispersion and better convergence: in particular, about half-a-

year prior to the time of the maximum realized velocity indicated by the horizontal dashed line, the prediction of this date by the renormalization method using the longer time series becomes very precise. Thus, a critical time close to the time of the velocity peak would have been predicted starting approximately half-a-year year from it. It is then not unreasonable to consider the velocity peak as a proxy for the critical time that the system would have exhibited in absence of a change of regime, since on its approach the largest internal stresses may develop and may fragment the block and modify the morphology of the landslide, thus resetting the geometry and some of the parameters of the model. In this scenario, we would thus expect that the time of the peak velocity should be not far from what would have been the critical time of catastrophic failure of the landslide.

We should however point out that the functional renormalization method used in this Appendix B does not work for the Vaiont landslide because of a technical instability whose fundamental origin is not understood by these authors. Technically, the numerical instability comes from the absence of alternating signs in the polynomial expansion at early times. This technical problem thus casts some shadow on the usefulness of the approach described here which is unable to tackle the regime which is undoubtedly unstable. This limitation suggests again the importance of working with several alternative and competing models, as further discussed in the following concluding section.

5   Discussion and conclusion

We have extended the quantitative analysis of our companion paper [1] on the displacement history for two landslides, Vaiont and La Clapière, to explore their potential predictability. Using a variety of techniques, we have tried to go beyond the time-independent hazard analysis provided by the standard stability analysis to include time dependent predictions. While our present inversion methods provide a single estimate of the critical time t_c of the collapse for each inversion, a better formulation should be to translate these results in terms of a probability of failure, as for instance done by Vere-Jones et al. [30].

Using the innovative concept of applying to landslides the state and velocity dependent friction law established in the laboratory and used to model earthquake friction, our inversion of this simple slider-block friction model shows that the observed movements can be well reproduced and suggest the Vaiont landslide (respectively La Clapière landslide) as belonging to the velocity weakening unstable (respectively strengthening stable) regime.

For the Vaiont landslide, the friction model provides good predictions of the time-to-failure up to 20 days before the collapse. A pure phenomenological model suggested by Voight [10] postulating a power law finite-time singularity $\dot{\delta} \sim 1/(t_c - t)$ with unit exponent obtains similar results up to 10 days before the collapse. Our approach can be seen as providing a physically-based derivation of this phenomenological model as well as a generalization to capture three other possible regimes.

For la Clapière landslide, the inversion of the displacement data for the accelerating phase 1983-1888 up to the maximum of the velocity gives $m < 1$, corresponding to the stable regime. The deceleration observed after 1988 implies that, not only is la Clapière landslide in the stable regime but in addition, some parameters of the friction law have changed, resulting in a change of sliding regime from a stable regime to another one characterized by a smaller velocity, as if some stabilizing process was occurring. Possible candidates for a change in landsliding regime include the average dip slope angle, the partitioning of blocks, new sliding surfaces and changes in interface properties. However, another possible interpretation is that this landslide was initially in the unstable regime, but did not reach the instability due to a change of geometry and of sliding surfaces. The best fit obtained with $m < 1$ for the accelerating phase 1983-1988 would then describe a transient regime between the unstable regime and the stable regime, due to a progressive change in the model parameters. This second scenario seems less parsimonious but cannot be completely excluded.

The present work has offered the novel conceptual framework and language of the slider-block model, which can be used to classify the relative merits and performance of other models. For an assessment in real time of the upcoming risks of a catastrophic failure, one should then consider both scenarios (stable versus unstable which are encoded respectively by the range of parameters $m < 1$ and $m > 1$ in the slider-block model) and test the data using the available associated theoretical models, some of which have been presented in this paper. Such an approach in terms of multiple scenarios [31, 32, 33] can help assess societal risks. A systematic exploration of such approaches will extend the preliminary investigation and results offered here.

A Appendix A: Functional renormalization group formulas for the friction law (9) and (10)

Consider an expansion as in (12) of an observable $x(t)$ in powers of a variable u given by $x_k(u) = \sum_{n=0}^{k} a_n u^n$. The method of algebraic self-similar renormalization constructs so-called "approximants", which are reconstructed functions that best satisfy the imposed asymptotic constraints while obeying criteria of functional self-similarity and of maximum stability in the space of functions [17, 18, 19]. These approximants are given by the following general recurrence formula for the approximate $x_k^*(u)$ of order k as a function of the expansion $x_{k-1}(u)$ up to order $k - 1$:

$$x_k^*(u) = \left[x_{k-1}^{-k/s}(u) - \frac{k \, a_k}{s} \, u^k \right]^{-s/k} . \tag{15}$$

The crossover index s is determined by the condition that the leading terms of the expansion of $x_k^*(t)$ as $t \to 0$ must agree with the expansion of $x_k(u)$.

For the friction model (9) and (10), the coefficients a_k in (12) and (15) are determined by the friction parameters and the initial conditions

$$a_0 = y_0, \tag{16}$$

$$a_1 = \theta_0^{-1} - S \, y_0^{1-m}, \tag{17}$$

$$a_2 = \frac{1}{2} S \, (m - 1) \, a_1 y_0^{-m}, \tag{18}$$

$$a_3 = \frac{1}{6} \alpha (m - 1) \left[-m \, a_1^2 \, y_0^{-m-1} + 2 a_2 \, x_0^{-m} \right], \tag{19}$$

$$a_4 = \frac{1}{24} S (m - 1) \left[(1 + m) \, m \, a_1^3 \, y_0^{-m-2} \right.$$
$$\left. - 6m \, a_2 \, a_1 y_0^{-m-1} + 6 a_3 \, y_0^{-m} \right], \tag{20}$$

where $y_0 = \theta(t = 0)/\theta_0$.

A.1 Case $m < 1$

As we see from (13), the natural expansion variable is $u = \exp\left(-\frac{t}{t^*}\right)$.

The first-order and simplest approximate is

$$x_1^*(u) = x^* \left(1 + cu\right)^{-s} = x^* \left(1 + c\exp\left(-\frac{t}{t^*}\right)\right)^{-s}, \tag{21}$$

with $x^* = 1/T$ where T is given by (11). The crossover amplitude c and the crossover index s are determined by the condition that the expansion of $x_1^*(t)$ as $t \to 0$ must agree with the first two terms of expression (12), leading to the following system of equations,

$$x^* \left(1 + c\right)^{-s} = x_0, \tag{22}$$

$$x_0 s\, c\, \frac{1}{t^*(1+c)} = a_1. \tag{23}$$

The crossover index s is then given by

$$s = -\frac{\ln\left(x_0/x^*\right)}{\ln\left(1+c\right)}, \tag{24}$$

while the crossover amplitude c satisfies the following equation:

$$\frac{\ln\left(x_0/x^*\right)}{\ln\left(1+c\right)} \frac{c}{(1+c)} = -\frac{a_1 t^*}{x_0}. \tag{25}$$

The second-order approximate is given by

$$\begin{aligned}
x_2^*(u) &= x^* \left[\left(1 + c_2 u\right)^{-s_2} + c_1 u^2\right]^{-s_1} \\
&= x^* \left[\left(1 + c_2 \exp\left(-\frac{t}{t^*}\right)\right)^{-s_2} + c_1 \exp\left(-\frac{2t}{t^*}\right)\right]^{-s_1}. \tag{26}
\end{aligned}$$

The crossover amplitudes c_1, c_2 and crossover index s_1 and s_2 are obtained from the condition that the expansion of $x_2^*(t)$ as $t \to 0$ must recover the first four terms of expression (12). The corresponding expressions are rather long and will not be presented here explicitly. Interestingly, for $m = 0$, the second-order approximate recovers the exact solution.

A.2 Case $m \geq 1$

In this case, the natural variable in the expansion is $u = t$. Our goal is to obtain the critical time t_c as a function of m. Using the crossover technique [19] for the two asymptotic expressions (12) at short time and (14) close to t_c, we obtain a sequence of approximants $x_1^*(t)$, $x_2^*(t), x_3^*(t)$ and $x_4^*(t)$ associated with a sequence of improving approximations for the critical time, $t_{c1}(m)$, $t_{c2}(m)$, $t_{c3}(m)$ and $t_{c4}(m)$. All approximants agree term-by-term with the corresponding short time expansion and lead to the critical behavior (14) as t goes to the corresponding critical time. The first-order approximate is

$$x_1^*(t) = x_0 \left(1 + \frac{a_1}{x_0} m\, t\right)^{1/m}, \text{ with } t_{c1} = -\frac{x_0}{m\, a_1}. \tag{27}$$

Interestingly, $x_1^*(t)$ coincides with the exact solution in the limit $m \to \infty$, which takes the form $x = x^* \left((x_0/x^*)^m - (t/t^*)\right)^{\frac{1}{m}}$.

In the next order, we obtain the second-order approximate

$$x_2^*(t) = x_0 \left[\left(1 + \frac{a_1}{x_0} t\right)^m + \frac{m\, a_2}{x_0} t^2\right]^{1/m}, \tag{28}$$

14

and t_{c2} is solution of the following equation

$$\left(1 + \frac{a_1}{x_0}\, t_{c2}\right)^m + \frac{m\, a_2}{x_0}\, t_{c2}^2 = 0 \ . \tag{29}$$

The third order approximate reads

$$x_3^*(t) = x_0 \left[\left(1 + \frac{a_1}{x_0}t + \frac{a_2}{x_0}t^2\right)^m + \frac{m\, a_3}{x_0}t^3\right]^{1/m} , \tag{30}$$

and t_{c3} satisfies the following equation

$$\left(1 + \frac{a_1}{x_0}\, t_{c3} + \frac{a_2}{x_0}t_{c3}^2\right)^m + \frac{m\, a_3}{x_0}\, t_{c3}^3 = 0 \ . \tag{31}$$

The fourth-order approximate is given by

$$x_4^*(t) = x_0 \left[\left(1 + \frac{a_1}{x_0}t + \frac{a_2}{x_0}t^2 + \frac{a_3}{x_0}t^3\right)^m + \frac{m\, a_4}{x_0}t^4\right]^{1/m} , \tag{32}$$

with t_{c4} solution of the equation

$$\left(1 + \frac{a_1}{x_0}t_{c4} + \frac{a_2}{x_0}t_{c4}^2 + \frac{a_3}{x_0}t_{c4}^3\right)^m + \frac{m\, a_4}{x_0}t_{c4}^4 = 0 \ . \tag{33}$$

Note that for $m = 1$, all approximants are identical and equal to the exact solution.

B Appendix B: Functional renormalization of polynomials expansions for the prediction of t_c as a function of the "present time" $t_{\max}$ for La Clapière landslide

This appendix present tests of the prediction of the time at which the velocity peaked, following the hypothesis discussed in the main text that the ensuing deceleration resulted from a change from $x_i < 1$ to $x_i > 1$ in the velocity weakening regime $B > A$. According to this interpretation, the first accelerating phase should be described by an increasing velocity $\propto 1/t_c - t$. The critical time t_c can be approximated by the time of the peak of the velocity, in other words, t_c is close to the inflection point of the displacement as a function of time.

Rather than using the version of the functional renormalization method described for the Vaiont landslide based on the slider-block equations of motion, we use here a simpler version that has been tested earlier in another rupture problem [20]. This choice is governed by the fact that we can not rely entirely on the friction model with fixed parameters since we know that a change of regime occurred. We thus follow a more general approach which is not dependent upon a specialized specification of the equations of motion. The previous investigation on a model system [20] developed theoretical formulas for the prediction of the singular time of systems which are a priori known to exhibit a critical behavior, based solely on the knowledge of the early time evolution of an observable. From the parameterization of such early time evolution in terms of a low-order polynomial of the time variable, the functional renormalization approach introduced by Yukalov and Gluzman [17] allows one to transform this polynomial into a function which is asymptotically a power law. The value of the critical time t_c, *conditioned* on the assumption that t_c exists, can then be determined from the knowledge of the coefficients of the polynomials. *Gluzman et al.* [20] have tested with success this prediction scheme on a specific example and showed that this approach gives

more precise and reliable predictions than through the use of the asymptotic power law model, but is probably not better than the true model when the later is known.

The input of the method is the inverse of La Clapière block velocity $\dot{\delta}$ as a function of time up to the "present time" $t_{\max}$. One starts with a simple polynomial fit of $1/\dot{\delta}$ as a function of time from some starting time up to $t_{\max}$. One then applies the functional renormalization method explained in [20] to this polynomial expansion. We restrict our analysis to expansions of up to second-order in time:

$$1/\dot{\delta} = 1 + b_1 t + b_2 t^2 \ , \tag{34}$$

where the zeroth-order coefficient b_0 has been put equal to 1 by a suitable normalization of the data.

The first order approximant for the inverse velocity reads [20]

$$F_1^*(t) = \left(1 - \frac{b_1}{s_1} t\right)^{-s_1} \ . \tag{35}$$

The second order approximant is

$$F_2^*(t) = 1 + b_1 t \left(1 - \frac{b_2}{b_1 s_2} t\right)^{-s_2} \ . \tag{36}$$

The exponents s_1 and s_2 are control parameters that are determined from an optimal stability criterion. We follow [20] and impose $s_1 = s_2 = s$, which is a condition of consistency between the two approximants. s is now the single control parameter, and plays the role of the critical exponent at the critical point t_c. The condition of the existence of a critical point is that both approximants $F_1^*(t)$ and $F_2^*(t)$ of the inverse velocity should vanish at $t = t_c$. This yields two equations determining t_c and s, which can be solved numerically.

The numerical estimates of (t_c, s) depends on the time interval over which the polynomial coefficients b_1 and b_2 are determined. Let $t_{\max}$ denote the last point used in the polynomial fit. Figure 12 shows the numerical estimate of t_c as a function of $t_{\max}$. More precisely, Figure 12 compares the prediction of a fit using a polynomial of order two in time to the inverse of the velocity (panel (a)) with the prediction of the renormalization approach (panel (b)).

We have also fitted a power law to the data to extract an estimate of t_c as a function of $t_{\max}$ and find an extremely unstable prediction where t_c fluctuates wildly ranging from two years before the end of 1987 to 25 years after 1987. Clearly, predicting the change of regime from a power law fit of the acceleration in the first phase of La Clapière is completely unreliable. In contrast, the renormalized approximants provide a more reasonable stable estimate.

References

[1] A. Helmstetter, D. Sornette, J.-R. Grasso, J. Andersen, S. Gluzman and V.F. Pisarenko, Slider-Block Friction Model for Landslides: Application to Vaiont and La Clapière Landslides, submitted to J. Geophys. Res. (2002)

[2] A. Bunde, J. Kropp and H.-J. Schellnhuber (Eds.), The Science of Disasters (Springer, Berlin, 2002).

[3] R.J. Geller, D.D. Jackson, Y.Y. Kagan and F. Mulargia, Science 275, 1616 (1997).

[4] W.J. Karplus, The heavens are falling : the scientific prediction of catastrophes in our time (New York: Plenum Press, 1992).

[5] D. Sornette, Proc. Nat. Acad. Sci. USA 99, 2522 (2002).

[6] D. Sornette, Why Stock Markets Crash: Critical Events in Complex Financial Systems (Princeton University Press, 2003).

[7] V.I. Keilis-Borok and A.A. Soloviev, eds., Nonlinear dynamics of the lithosphere and earthquake prediction (New York: Springer, 2003).

[8] E. Hoek and J. W. Bray, *Rock slope engineering*, 3rd Edn (rev), Institution of Mining and Metallurgy and E&FN Spon, London, pp 358, 1997.

[9] E. Hoek and E. T. Brown, *Underground excavation in rock*, Institution of Mining and Metallurgy, London, 1980.

[10] B. Voight, Nature 332, 125, 1988.

[11] T. Fukuzono, Method for predicting the failure time of a slope, *Proceedings of the 4th Int. Conf. Field Workshop on Landslides*, National Research Center for Disaster prevention, Tokyo, 145-150, 1985.

[12] R.K. Bhandari, Some lessons in the investigation and field monitoring of landslides, *Proceedings 5th Int. Symp. Landslides lausanne 1988, eds C. Bonnard , 3*, 1435-1457, Balkema, 1988.

[13] J. Dieterich, Pure Appl. Geophys. 116, 790, 1978.

[14] A.L. Ruina, J. Geophys. Res., 88, 10359, 1983.

[15] Y. Huang, A. Johansen, M. W. Lee, H. Saleur and D. Sornette, J. Geophys. Res. 105, 25451, 2000.

[16] Erismann, T.H. and G. Abele, *Dynamics of Rockslides and Rockfalls*, Springer, 2000.

[17] V.I. Yukalov and S. Gluzman, Phys. Rev. E 55, 6552, 1997.

[18] S. Gluzman and V. I. Yukalov, Phys. Rev. E 55, 3983, 1997.

[19] S. Gluzman and V. I. Yukalov, Phys. Rev. E 58, 4197, 1998.

[20] S. Gluzman, J. V. Andersen and D. Sornette, Computational Seismology 32, 122, 2001.

[21] S. Gluzman and D. Sornette, Phys. Rev. E 66, 016134, 2002.

[22] D. Sornette and A. Johansen, Quantitative Finance 1, 452, 2001.

[23] J.P. Follacci, P. Guardia and J. P. Ivaldi, La Clapière landslide in its geodynamical setting, *Bonnard eds , Proc. 5th Int. Symp. on Landslides, 3*, 1323, 1988.

[24] J.P. Follacci, L. Rochet and J.-F. Serratrice, Glissement de La Clapière, St Etienne de Tinée, Synthèse des connaissances et actualisation des risques, *rapport 92/PP/UN/I/DRM/03/AI/01, Ministère Environnement, 76*, 1993.

[25] Susella, G. and F. Zanolini, Risques générés par les grands mouvements de terrains, *eds, Programme Interreg 1, France-Italie*, 207 pp., 1996.

[26] E. David and ATM, Glissement de La Clapière, St Etienne de Tinée, Etude cinématique, géomorphologique et de stabilité, *rapport CETE Nice*, France, 88 pp., 2000.

[27] M. Rat, Difficulties in forseeing failure in landslides – La Clapiére, French Alps, *Proceedings 5th Int. Symp. Landslides lausanne 1988, eds C. Bonnard, vol 3*, 1503-1504, Balkema, 1988.

[28] V.F. Pisarenko, A. A. Lyubushin, S. Canu, M. F. Kanevsky, E. A. Savelieya, V. V. Demianov, M. V. Bolgov, T. A. Rukavishnikova, and I. V. Zalyapin, Statistical methods for river's runoff forecast, 2002, submitted to *Water Resources Research*. (this paper was presented at the 4-th INTAS Interdisciplinary Symposium on Physical and Chemical Methods in Biology, Medicine and Environment, Moscow, May 30 - June 3, 2001).

[29] Guglielmi, J., and J. M. Vengeon, Interrelation between gravitational patterns and structural fractures La Clapière, French Alps, submitted to *Geomorphology*, 2002.

[30] D. Vere-Jones, D., R. Robinson and W. Z. Yang, Geophys. J. Int. 144, 517, 2001.

[31] L.A. Smith, C. Ziehmann and K. Fraedrich, Quarterly J. Royal Meteor. Soc., 125, 2855, 1999.

[32] V.I. Yukalov and S. Gluzman, Int. J. Mod. Phys. B 13, 1463, 1999.

[33] C. Ziehmann, C., L. A. Smith and J. Kurths, Phys. Lett. A 271, 237, 2000.
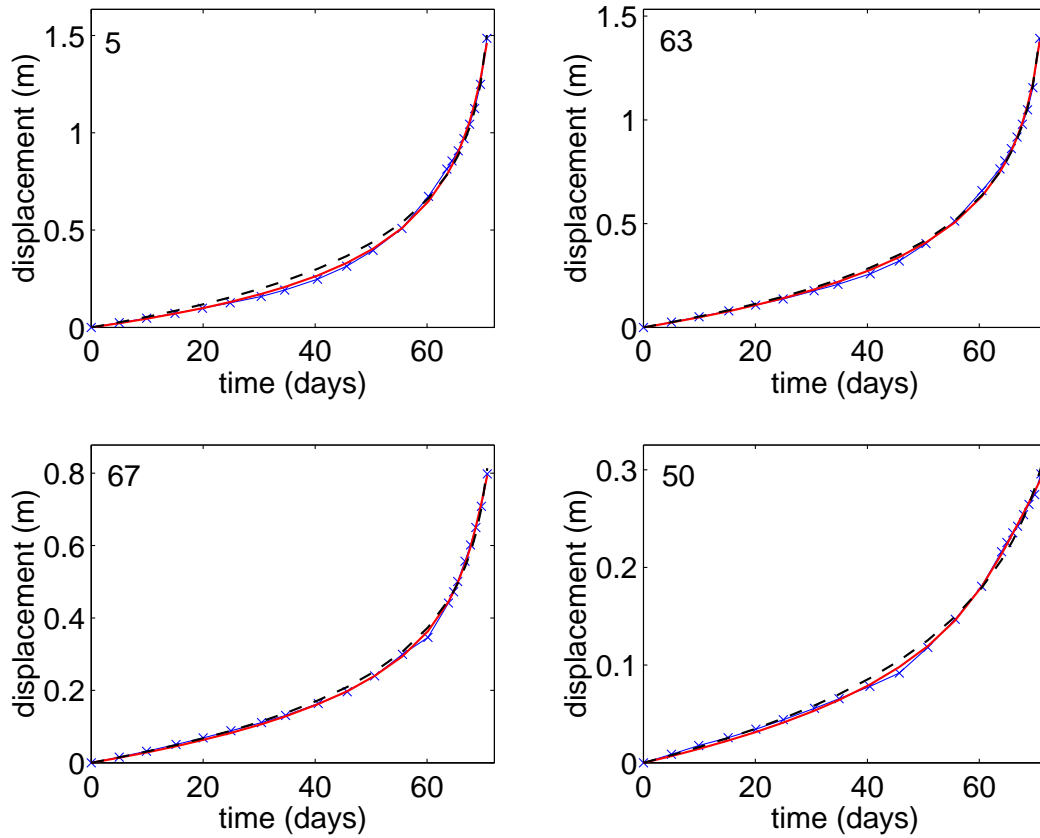
Figure 1: For each of the four Vaiont benchmarks, the cumulative displacement data is fitted with the slider-block model with the state and velocity friction law (10) and (9) by adjusting the set of parameters m, D/T and the initial condition of the state variable x_i. The data is shown as the crosses linked by straight segments and the fit is the thin continuous line. The fitted m are respectively $m = 0.99$ (benchmark 5), $m = 0.85$ (benchmark 63), $m = 0.68$ (benchmark 67) and $m = 0.17$ (benchmark 50). The fits with the slider-block model obtained by imposing the value $m = 1.5$ are shown with the dashed line for comparison.
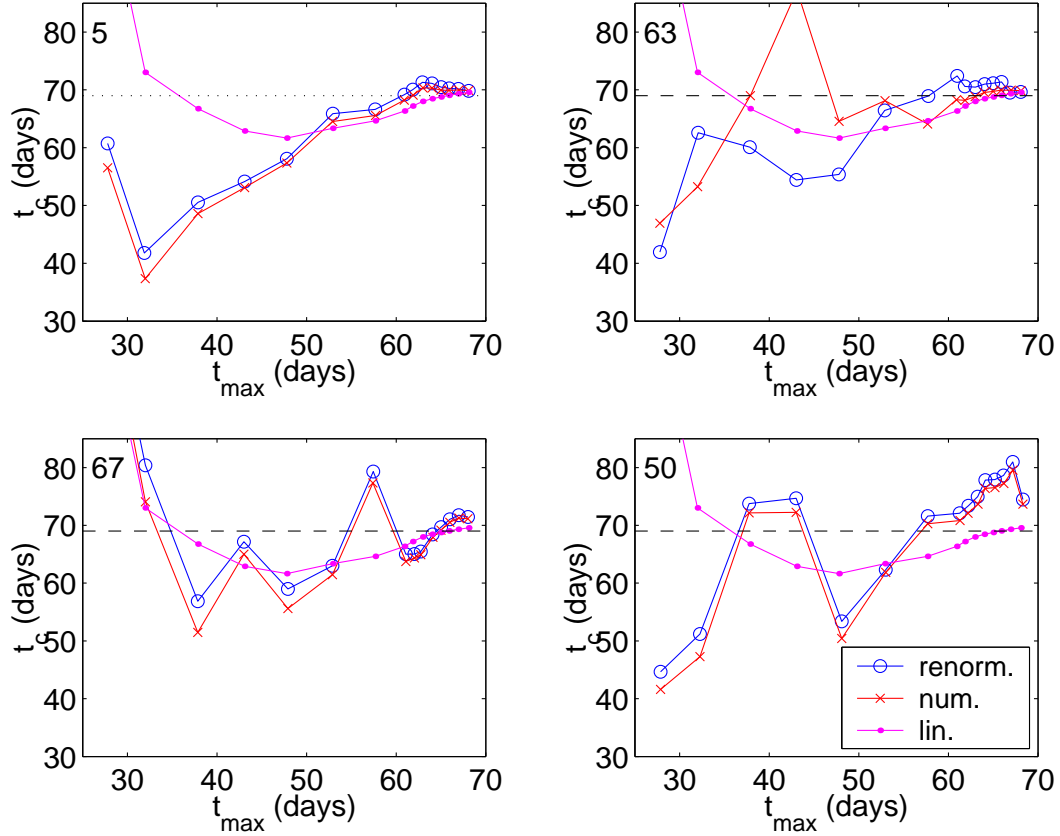
Figure 2: Predicted critical time t_c as a function of the "present time" t_{max} (last point used for the fit) for all four benchmarks of the Vaiont landslide, using three different methods of prediction described in the text: renormalization method (circles), numerical evaluation of the friction model (10) (crosses), and linear regression of the inverse velocity as a function of time performed by removing the first point (early time) of the curve and using a weight proportional to the velocity (dots). The horizontal dashed line indicated the true critical time $t_c = 69.5$ days (for an arbitrary origin of time from which the fits are performed to the catastrophic landslide. All methods impose $m > 1$, but in some cases a better fit may be obtained in the stable regime $m < 1$.
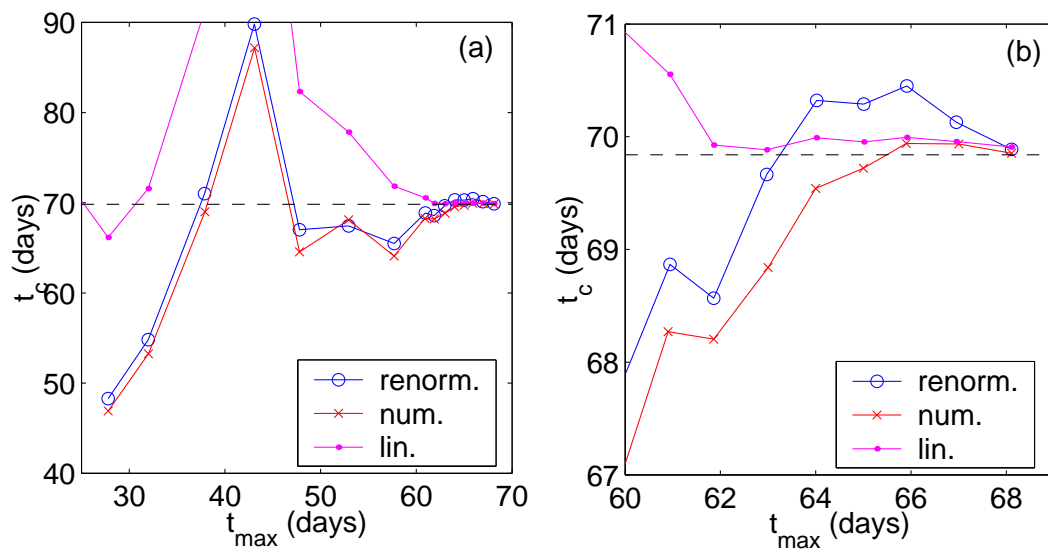
Figure 3: Same as Figure 2 for a synthetic data set with the same parameters and noise as those obtained for benchmark 5 of the Vaiont landslide, using the same three different methods of prediction. The right panel is a zoom of the left panel close to t_c. The horizontal dashed line indicated the true critical time $t_c = 69.8$ of the catastrophic landslide.
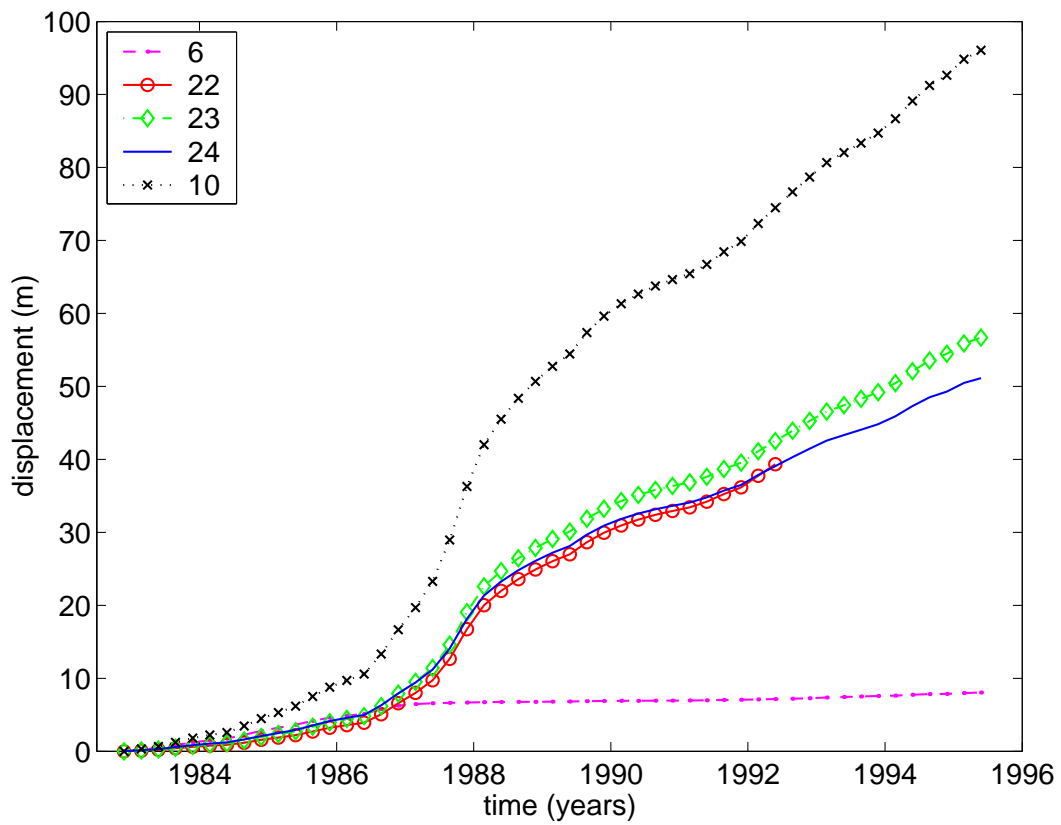
Figure 4: Displacement for the 5 benchmarks on La Clapière used in this study.
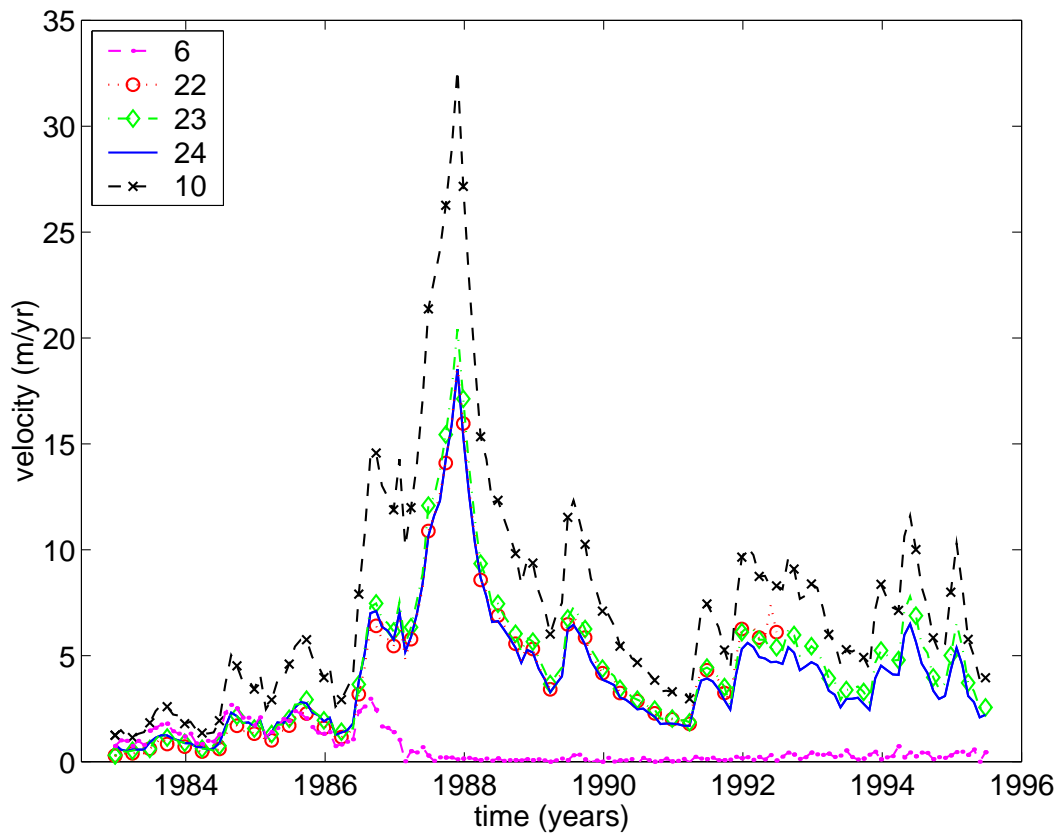
Figure 5: Velocity for the same data as shown in Figure 4. Annual fluctuations of the velocity is due to the seasonal variations of the precipitations.
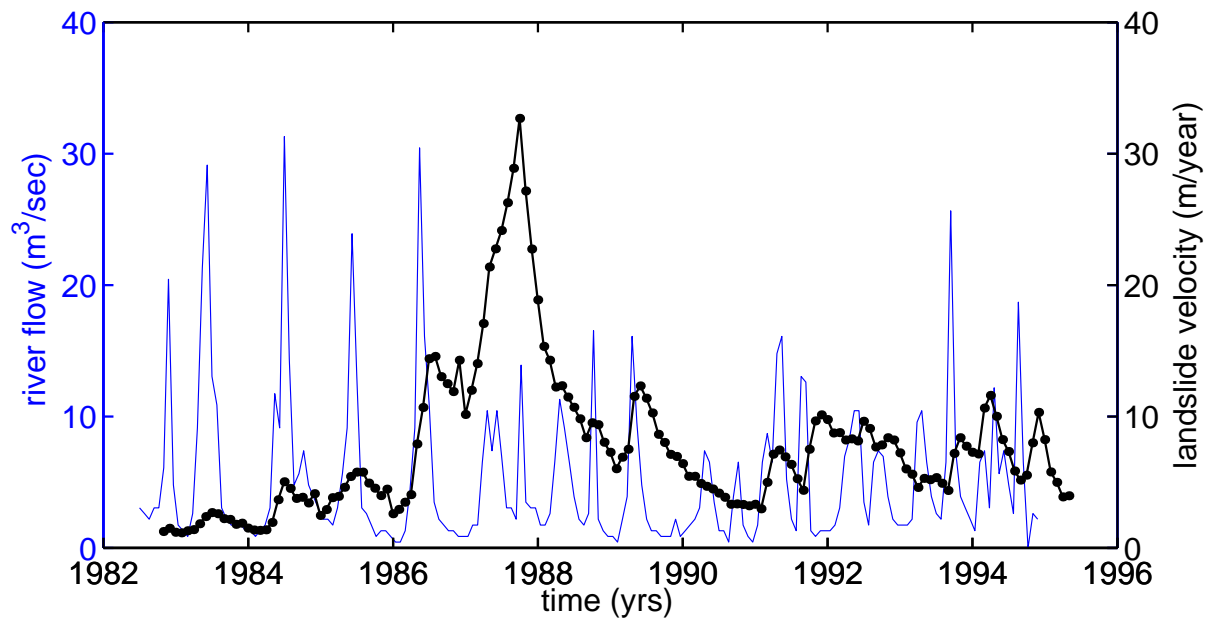
Figure 6: Velocity pattern for benchmark 10 of La Clapière landslide (solid line and dots) and flow rates (thin solid line) of the Tinée river on the 1982-1995 period. Because the Tinée river runs at the basis of the La Clapière landslide, the river flow rate reflects the water flow within the landslide [24, 25]. The flow rates are measured at St Etienne village, 2 km upstream the landslide site. There is no stream network on the landslide site. The Tinée flow drains a 170 km^2 basin. This tiny basin is homogeneous both in terms of slopes and elevation (in the 1000-3000 m range). Accordingly the seasonal fluctuations of the river flow is admitted to reflect the evolution of the amount of water that is available within the landslide slope due to rainfalls and snow melting. Data from *CETE*, [1996].
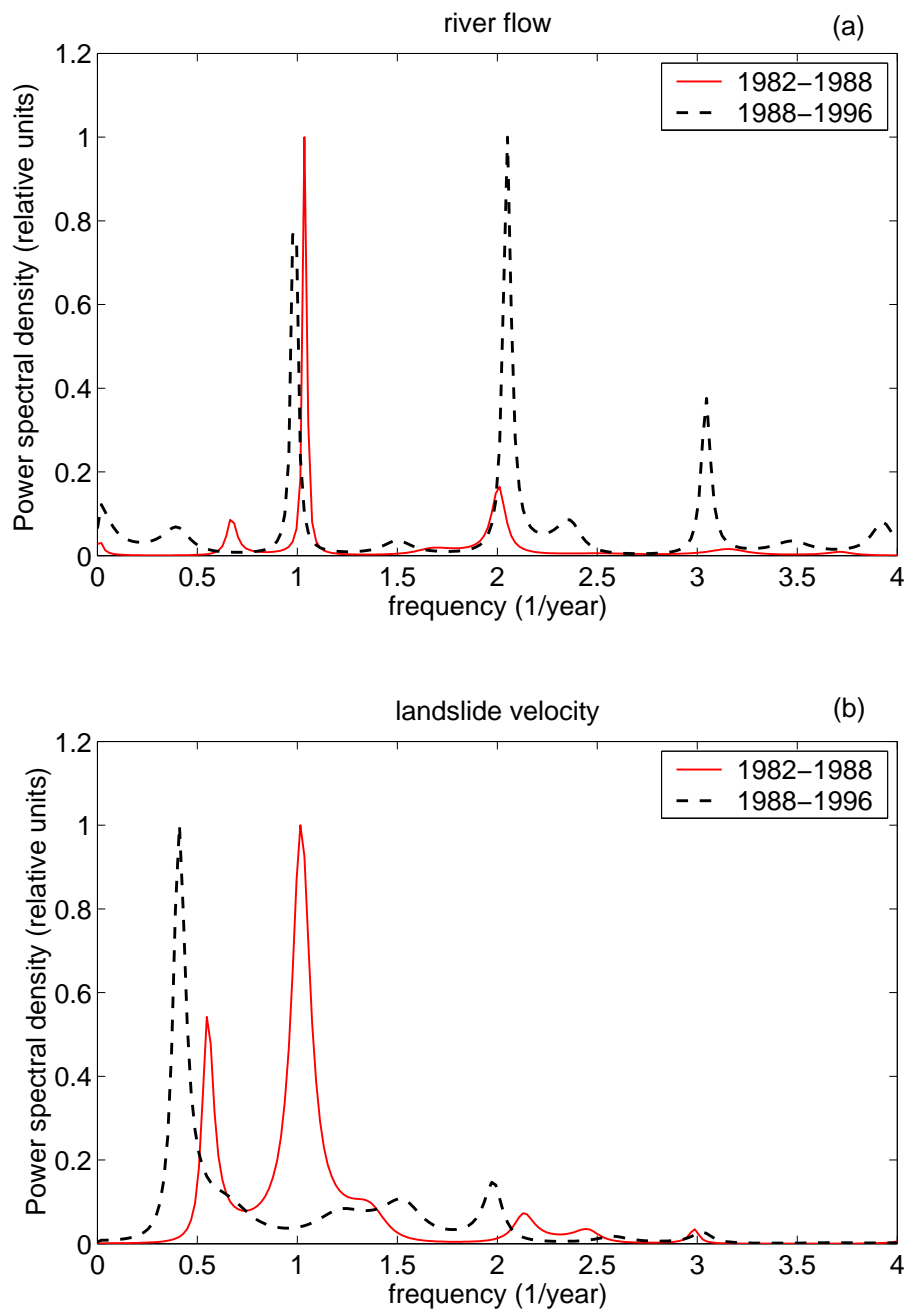
Figure 7: Top panel: Burg's power spectrum of the flow rates of the Tinée river on the 1982-1988 and on the 1988-1996 periods which are aggregated from the periods shown in figure 6. Bottom panel: Burg's power spectrum of the detrended velocity residuals for the same two periods.
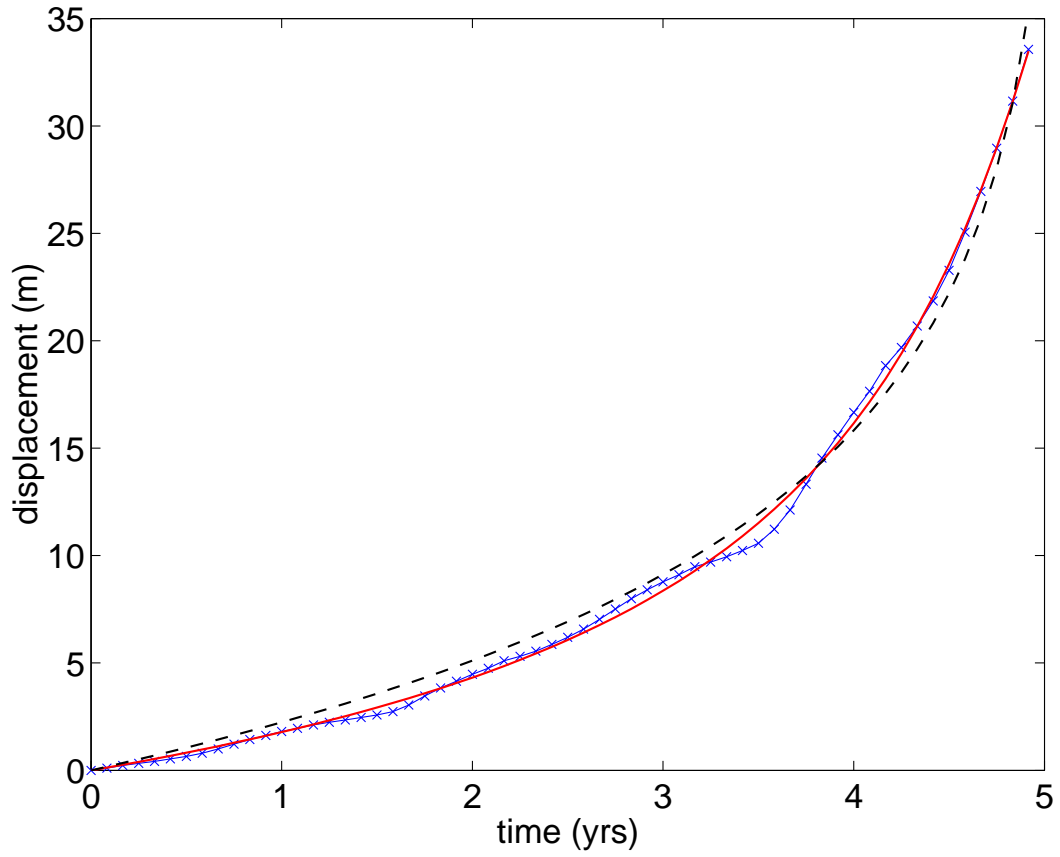
Figure 8: Displacement for benchmark 10 of la Clapière landslide (crosses) and fit using the friction model. The best fit gives $m = 0.98$ (black line). The gray line shows the best fit obtained when imposing $m = 1.5$ for comparison.
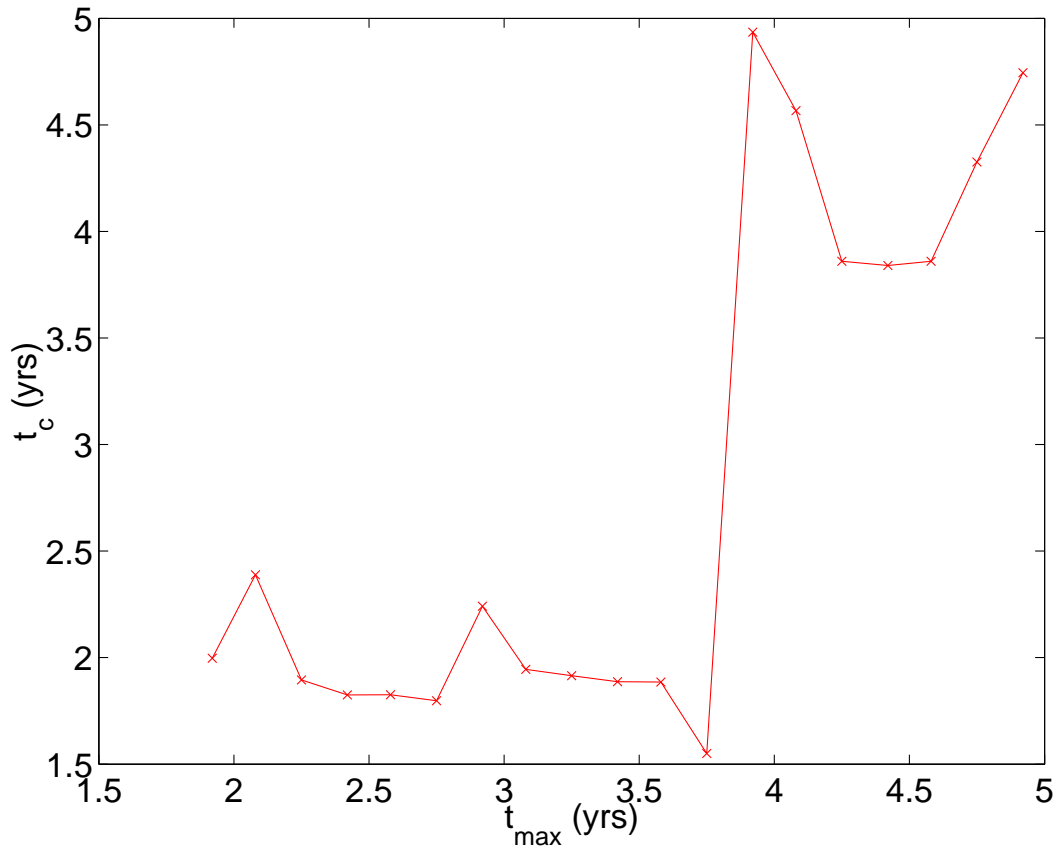
Figure 9: Predicted value of the time t_c of the inflection point of the velocity for La Clapière landslide, using a fit of the displacement data with the friction model. All points correspond to the stable regime $m < 1$. In this regime there is no finite-time singularity of the velocity but a transition from an accelerating sliding to a stable sliding for times larger than the inflection point t_c. This parameter is poorly constrained by the fit and increases with the time of the last point t_{max} used in the fit.
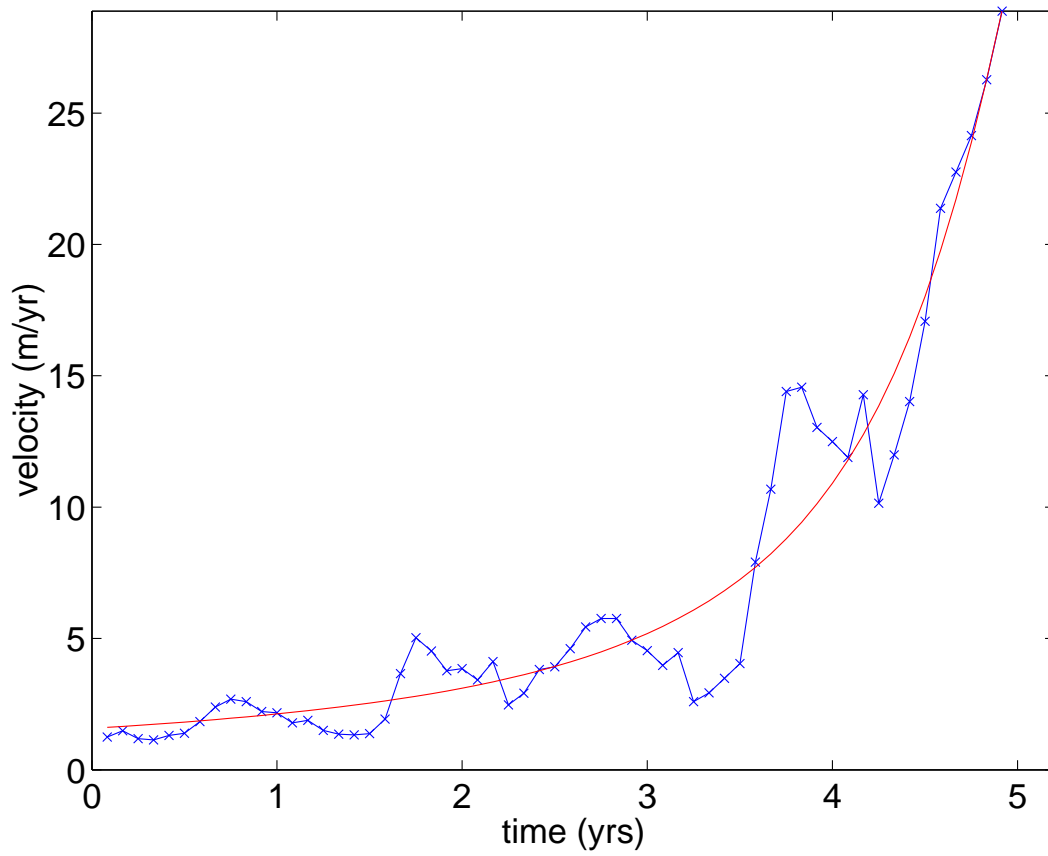
Figure 10: Velocity for benchmark 10 of la Clapière landslide (crosses) and fit of the velocity data with the friction model. The best fit gives $m = 0.99$ (black line).
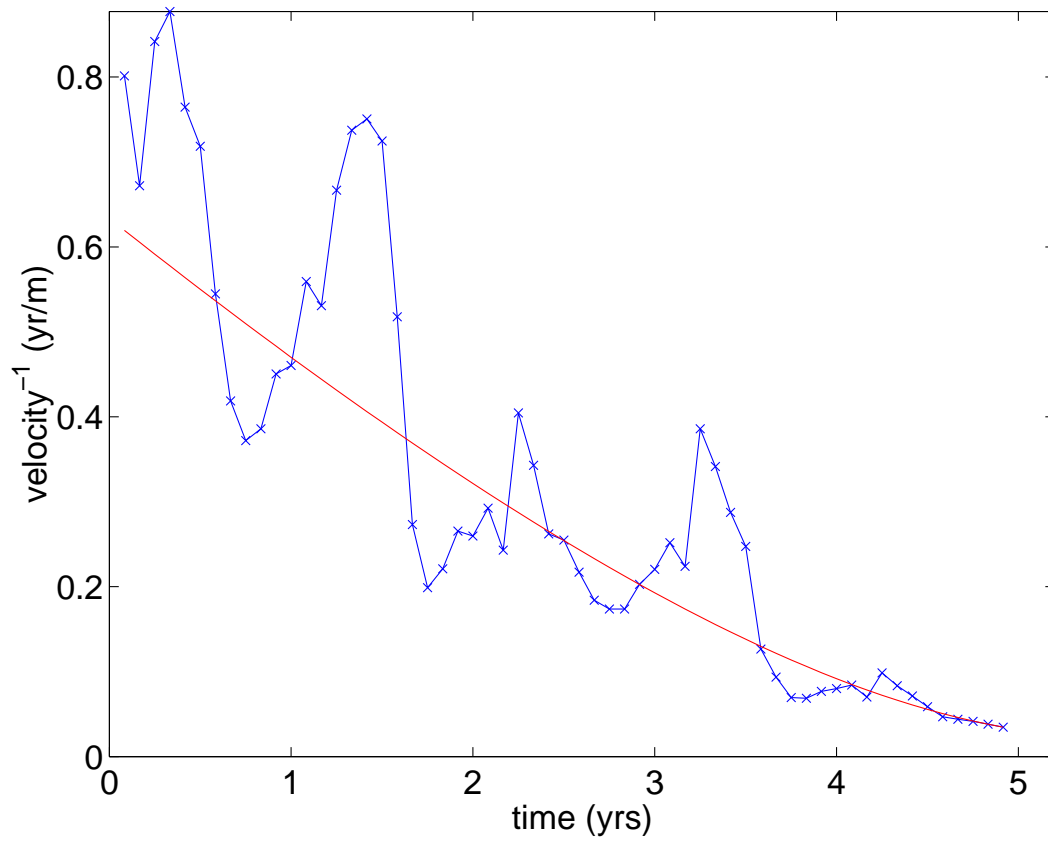
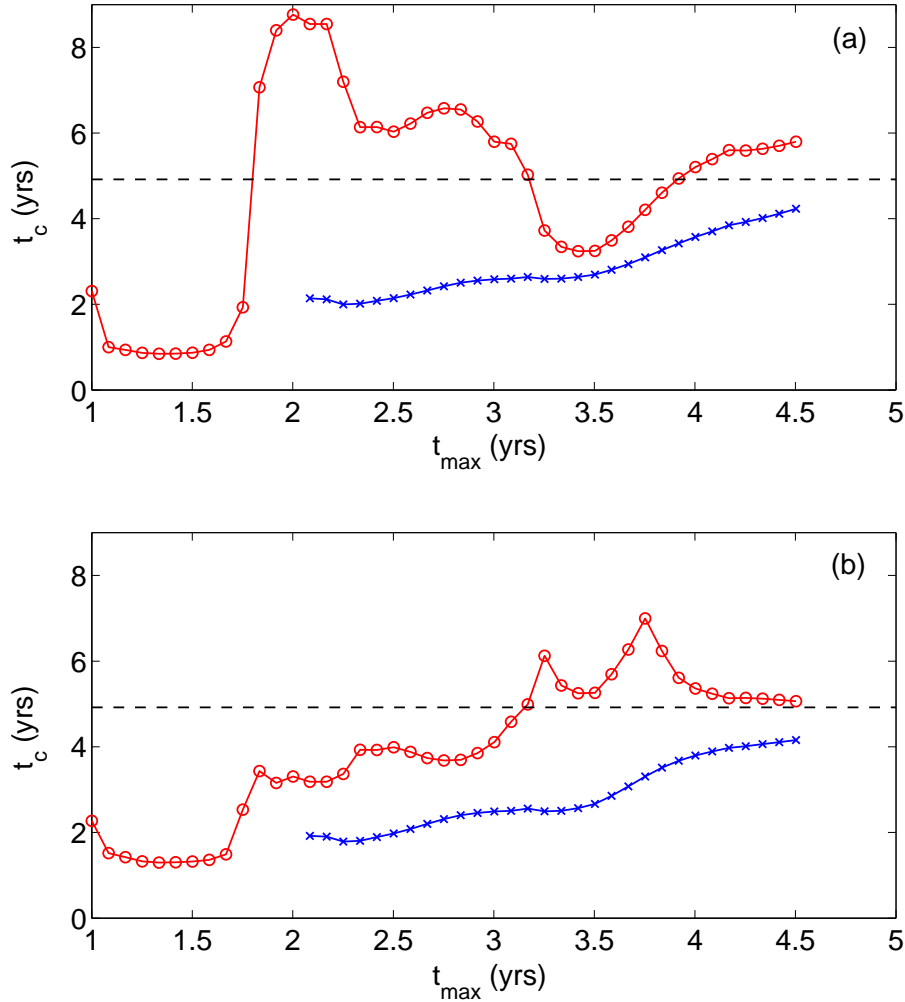Figure 11: Same as Figure 10 showing the inverse of the velocity.

Figure 12: Panel (a): prediction of a critical time using a fit with a polynomial of order two in time to the inverse of the velocity; panel (b): prediction of the renormalization approach described in Appendix B. In each panel, two curves are presented corresponding to two different starting points of the data taken into account in the predictions: the leftmost points correspond to the first date taken into account in the predictions; the predictions corresponding to the crosses $\times$ use approximately two years fewer data than the predictions shown with the open circles. The abscissa $t_{\max}$ is the running "present time", that is, the last time of the data taken into account to issue a prediction. The maximum realized velocity occurred at a time indicated by the horizontal dashed line. This time is thus a proxy for the ghost-like critical time of the landslide.